Finite Control Set – Model Predictive Control of a Nine Level Packed U Cell Grid Connected Multilevel Inverter

ALAA'ABUQUBAITA[1], SAMEER KHADER[1], ABDEL KARIM DAUD[1],HAMZA MAKHAMREH[2]
[1]Power Electronics Research Unit,
[1]Palestine Polytechnic University,
Hebron, PALESTINE
[1]sameer@ppu.edu
[2]Eastern Mediterranean University, CYPRUS

Abstract: - This paper describes a photovoltaic-grid connected Nine Level Packed U Cell (PUC9) topology using a Finite Control Set – Model Predictive Control (FCS-MPC) technique. The proposed system is a single-phase multilevel inverter, with four pairs of switches that work in a complementary matter, one DC source and two flying capacitors connected to the grid through a filtering inductor. This topology has the ability to generate nine different voltage levels with less number of active and passive components comparing with conventional multilevel inverter topologies. The proposed control technique (FCS-MPC) aims at reducing the total harmonic distortion (THD) of the grid injected current while balancing the capacitors' voltages at their nominal reference values. Robustness analysis of the proposed model including the effect of a step change in the injected current into the grid, parameters' mismatching, and grid voltage sag and swell have been conducted on a single phase low power (PUC9) inverter. Theoretical analysis, mathematical modelling and simulation results using MATLAB/SIMULINK software are presented in this paper.
The obtained THD of the injected current for the proposed model is 1.13% and the capacitors' voltages error is less than 5%.

Key-Words: -Multi Level Inverter, Genetic Algorithm, Packed U Cell Inverter, Total harmonic Distortion

1 Introduction

Nowadays, multilevel inverters (MLIs) are in rapid development and have become a very useful solution for renewable energy resources applications due to its ability to deal with different power rating, switching semiconductors, operating frequency, and applied voltage and current [1].

There are hundreds of publications dealt with multilevel converter technology and pointed to the importance of using this technology for high-power converters.

The most applied topologies are Cascaded H-Bridge (CHB), Flying Capacitor (FC), Neutral-Point Clamped (NPC), and Packed U-Cells (PUC) inverters. Figure1 shows the general configuration of MLIs integrated with the local electrical grid, where the PV generators can be one or more connected is such a way to form voltage levels in combination with connected capacitors [2].

In comparison with conventional inverters, MLIs are characterized with low total harmonic distortion; lower switching frequency, high power rating and less electromagnetic interference in addition to decreased switching losses.

PUC inverter classified as FC inverter has many advantages compared with other MLI topologies such as high power quality, ability and flexibility in the multilayer voltage synthesis, simple construction, reduced number of switches and DC sources, reliability, and less cost.

There are many control methods proposed to control PUC inverter, in [3] a novel six band hysteresis controller were proposed, which has a fast dynamic and robust behavior, but it can't deal with variable switching frequency.

In [4] the authors proposed a 14-band hysteresis controller to control a 16-level PUC inverter. In [5,6] the authors used two proportional-integral (PI) to control the capacitor voltage at the desired value, and the gate signals were generated using multicarrier and reference voltage comparison.

Model Predictive Control (MPC) is one of control techniques that used for power engineering, in the past, it was not used widely due to high computational cost, but recently, the rapid development in digital signal processors have become the common solution [7-12].

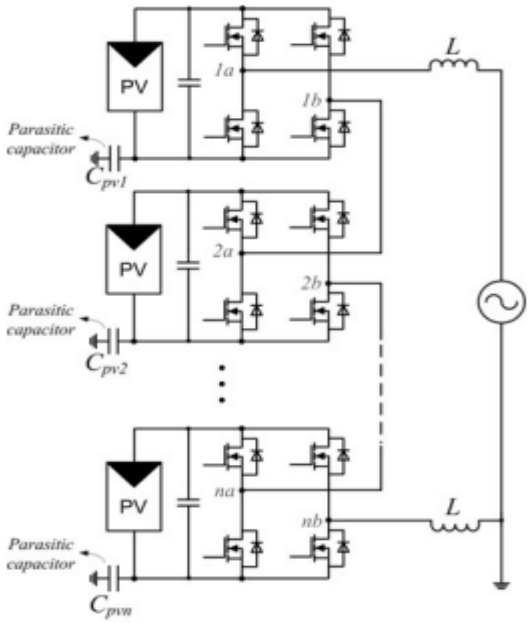

Fig.1: General circuit configuration for Grid-tie MLIs inverter.

2 Mathematical Modeling

2.1 Principle of operation of PUC9

This model is very similar to seven levels PUC inverter, but one pair of switches and one capacitor were added. The THD of the output voltage is expected to decrease due to the generated additional voltage level. Furthermore, the stress on the switches decreased as well because of limited amount of voltage that being handled by the switch as shown on Fig.2, [13-17].

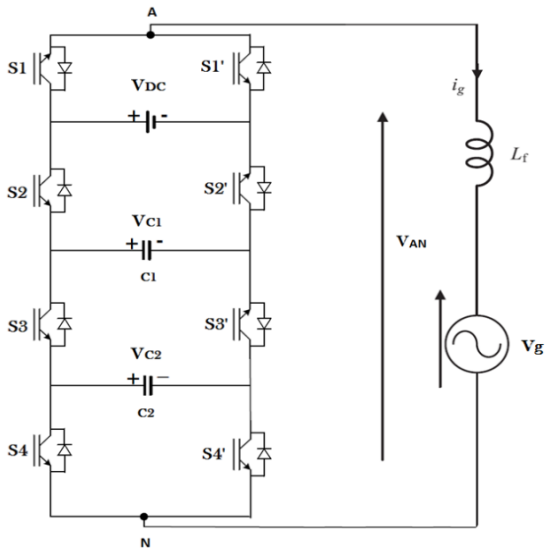

a) Circuit configuration with grid integration.

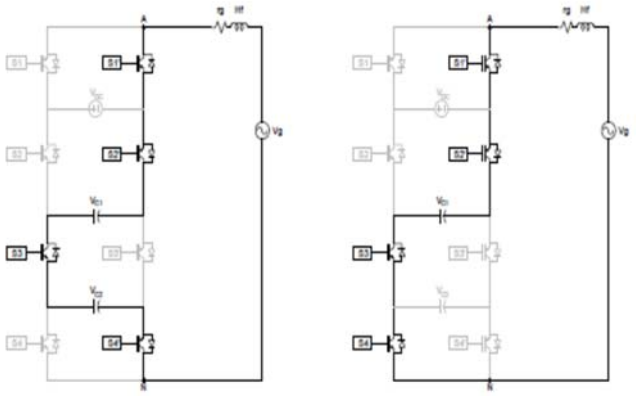

b) Configurations for state 7 and 8.

Fig.2: Nine-level PUC multilevel inverter topology.

Where it can be observed that PUC9 requires one PV source presented as V_{DC}, 8 switches and 2 capacitors with 16 combinations that make it competitive to other MLIs.

The proposed model has four pairs of switches(S_1,S_1'), (S_2,S_2'), (S_3,S_3'), and (S_4,S_4') triggered in a complementary matter, let Sx $\subseteq${0,1}, where x{1,2,3,4} and the obtained combinations are stated in table 1.

$$Sx = \begin{cases} 1, & if\ Sx\ is\ ON \\ 0, & if\ Sx\ is\ OFF \end{cases}; \qquad (1)$$

Where, V_{DC} is the voltage of the single source of the PV generator; $V_{C1}$and V_{C2} are the voltages of first and second capacitors respectively; and V_{AN} is the inverter output voltage. The proposed model generates 9 voltage levels (0, ±E, ±2E, ±3E, ±4E), where E= V_{DC}/4 which presents the reference voltage. The rated value of the DC voltage is V_{DC} = 4E, while V_{C1} = 2E and V_{C2} = E.

In the proposed model the grid current ig(t) must track the grid current reference, in addition to that , also the capacitors voltage V_{C1}(t) and V_{C2}(t) must be maintained at their nominal voltage values.

The generated output voltage of this inverter depends on the proposed voltage reference E and on the switching states with values presented in table 1, where the abbreviations **B** stands for bypass, **C** for charging &**D** for discharging.

Table1: Switching states and voltage of PUC9 multilevel inverter

Stat	S1	S2	S3	S4	Vout	Van	C1	C2
1	0	0	0	0	0	0	B	B
2	0	0	0	1	-E	$-V_{C2}$	B	C
3	0	0	1	0	-E	$-V_{C1}+V_{C2}$	C	D

4	0	0	1	1	-2E	$-V_{C1}$	C	B
5	0	1	0	0	-2E	$-V_{DC}+V_{C1}$	D	B
6	0	1	0	1	-3E	$-V_{DC}+V_{C1}-V_{C2}$	D	C
7	0	1	1	0	-3E	$-V_{DC}+V_{C2}$	B	D
8	0	1	1	1	-4E	$-V_{DC}$	B	B
9	1	0	0	0	4E	V_{DC}	B	B
10	1	0	0	1	3E	$V_{DC}-V_{C2}$	B	C
11	1	0	1	0	3E	$V_{DC}-V_{C1}+V_{C2}$	C	D
12	1	0	1	1	2E	$V_{DC}-V_{C1}$	C	B
13	1	1	0	0	2E	V_{C1}	D	B
14	1	1	0	1	E	$V_{C1}-V_{C2}$	D	C
15	**1**	**1**	**1**	**0**	**E**	**VC2**	**B**	**D**
16	1	1	1	1	0	0	B	B

2.2 Mathematical model of PCU9

Refer to Fig.1, and by applying Kirchhoff current and voltage laws the relations between grid current $i_g(t)$, capacitors voltages $V_{C1}(t)$,$V_{C2}(t)$, and the switching states Sx can be expressed as follow [18, 19]:

$$C1\ \frac{dV_{C1}}{dt} = (S3 - S2)\ x\ ig(t) \tag{2}$$

$$C2\ \frac{dV_{C2}}{dt} = (S4 - S3)\ x\ ig(t) \tag{3}$$

$$\begin{aligned} Lf\ \frac{dig(t)}{dt} = {} & (S1 - S2)\ x\ V_{DC}(t) \\ & + (S2 - S3)\ x\ V_{C1}(t) \\ & + (S3 - S4)\ x\ V_{C2}(t) \\ & - Vg(t) \end{aligned} \tag{4}$$

Where, C1 & C2 are model capacitors; V_{DC} is the source voltage; V_{C1} and $V_{C2}$are the capacitor voltages respectively; S_1, S_2, S_3, S_4 are switching states; L_f is the filter inductance; Vg(t) and ig(t) are grid voltage and current .

2.3 Mathematical modeling of FCS-MPC technique

Finite Control Set Model Predictive Control (FCS-MPC) is one of the most used control techniques that gives an optimal solution for related control problem by calculating the control action at each sampling time. The applied approach uses a dynamic strategy to forecast the future behavior from the current system state. So an optimal control solution will be generated.

The main advantage of this method is that the switching actions are considered as constraints on the control input of the system, as a result for that, the modulation levels are not required. [21, 22].

Fig. 3 shows the general control scheme for FCS-MPC.

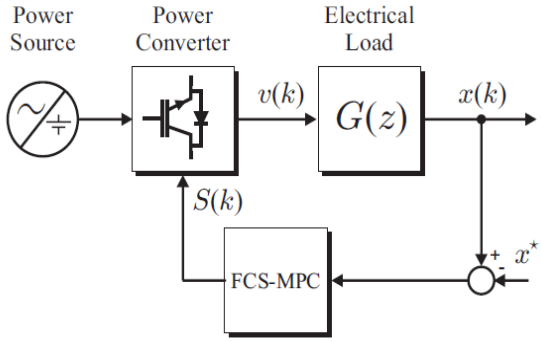

Fig.3: General control scheme for FCS-MPC.

Nowadays, MPC is used in several technical control applications [22-25], because it can deal with multivariable control, and unstable systems. However, MPC standard method does not care to the variation range of input and output, which leads to less tracking capabilities.

In general, MPC has the following main components:

- Prediction model
- Objective function
- Optimizing algorithm

The main challenge for the control method used in this paper is to keep the voltages of the capacitors at their rated voltages while tracking the grid current reference. Another important issue, that any change in one of the controlled parameters (such as capacitors' voltages or grid current) should affect the rest of parameters, which in turn complicating the control decisions.

The proposed solution in this research is to normalize the state variables by calculating the maximum variations of the state variables. These variations should be used as additional optimization criteria in the cost function calculation.

2.3.1 Model Prediction Control

The main idea for the control technique of this research is to predict the grid current (i_g^{k+1}) and capacitors' voltages (V_{C1}^{k+1}, V_{C2}^{k+1}) for each switching state (voltage vector generated by the inverter) in the means of discrete equations of the system state variables.

In order to simplify the model, the state variables' paths can be considered as rectilinear for a small sampling time.

So the state variable that given in equations (2),(3) and (4) will be approximated for each sampling time Ts using the following equation

$$x^{k+1} = x^k + \dot{x}(t).Ts \qquad (5)$$

Now, the prediction of the state variables at (k+1) sample of time in terms of the recent sample (k) are expressed as follow:

$$V_{C1}^{k+1} = V_{C1}^k + (S3 - S2)\frac{Ts}{C1} i_g^k \qquad (6)$$

$$V_{C2}^{k+1} = V_{C2}^k + (S4 - S3)\frac{Ts}{C2} i_g^k \qquad (7)$$

and,

$$i_g^{k+1} = i_g^k + (S1 - S2)V_{DC}^k + (S2 - S3)V_{C1}^k + (S3 - S4)V_{C2}^k - V_g^k \qquad (8)$$

2.3.2 State variables normalization

MPC technique does not matter to the variation ranges of the parameters (voltage and current). The main objective of this technique is to reduce the error between the reference and measurement, so it will select the switching state that gives the minimum error.

Before calculating the cost function, a normalized factor is proposed by calculating the maximum variations of the state variables (ΔV_{C1max}, ΔV_{C2max} and Δi_{gmax}) as follow:

$$\Delta V_{C1}max = \frac{2ig}{C1} Ts \qquad (9)$$

$$\Delta V_{C2}max = \frac{2ig}{C2} Ts \qquad (10)$$

$$\Delta i_g max = \frac{V_{AN}}{Lf} Ts \qquad (11)$$

2.3.3 Calculation of cost function

The main objective of the cost function is to minimize the difference between the predicted state variables ($V_{C1}^{k+1}, V_{C2}^{k+1}$ and i_g^{k+1}) and there references' values. Thus, the cost function can be expressed as:

$$g = \left|\frac{V_{C1}^* - V_{C1}(k+1)}{\Delta V_{C1}max}\right| + \left|\frac{V_{C2}^* - V_{C2}(k+1)}{\Delta V_{C2}max}\right| + \alpha\left|\frac{i_g^* - i_g(k+1)}{\Delta i_g max}\right| \qquad (12)$$

Where V_{C1}^* is the rated voltage of the first capacitor C_1 ($V_{C2}^* = 2E$), V_{C2}^* is the rated voltage for C2 ($V_{C2}^* = 3E$), i_g^* is the reference current, andα is the weighting factor that can be adjusted to get the desired results of the model [26]. Figure 4illustrates the proposed control strategy for PUC9 inverter.

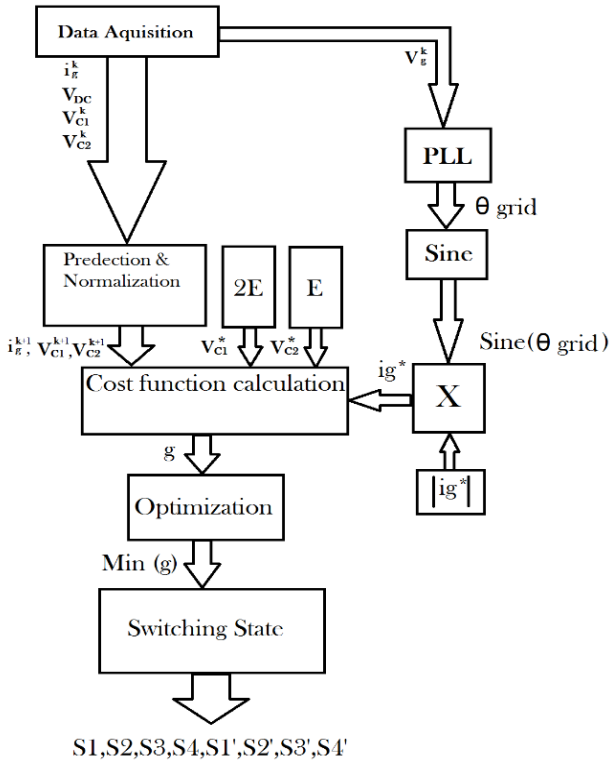

Fig.4: FCS-MPC strategy for PUC9 inverter

3 Simulation Results

The simulation model is built using MATLAB/SIMULINK environment [27], where the PV- grid connected model is displayed on Fig.5, while Fig.6 illustrates all the system modules. The simulation is conducted for real system parameters stated in table 2.

Table 2: Initial circuit parameters

Parameter	Value
Grid-side parameters	
Line to neutral voltage, Vrms, V	220
Frequency f, Hz	50
Phase shift θ, dg	0
Filter parameters	
Resistancerg,Ω	0.01
InductanceLf,mH	2.5
Inverter parameters	
Input DC voltageV_{DC} ,V	400
Desired voltage of C1, V_{C1},V	200
Desired voltage of C2, V_{C2},V	100
Capacitance of C1,mF	7
Capacitance of C2, mF	1
Number of voltage levels, n	9
Sampling time Ts, µs	25
Output rated power Po, kW	5

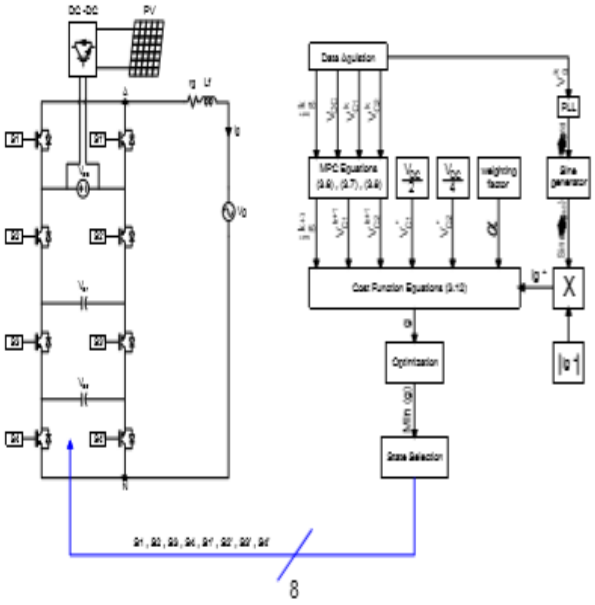

Fig.5: PV- Grid connected model.

3.1 Weighting factor (α) tuning

Weighting factor plays a vital role in the inverter performance and used to achieve the desired performance and the stability for this proposed model. The tuning of α must be done based on minimizing the total harmonic distortion (THD) of the grid current waveform and the error on the capacitors' voltages (V_{C1} and V_{C2}).

Attention to be paid that THD of 3the grid current, V_{C1} and V_{C2} voltage errors are considered as performance indicators for α value selection.

Fig. 7 illustrates the effect of varying weighting factor (α) on the performance indicators THD, V_{C1} and V_{C2}. Note that as α increases V_{C1} and V_{C2} error voltage increases, but THD is fluctuating between 3.07% and 1.31%. The optimum value of α is selected based on the minimum value of THD where α=0.22, and THD becomes 1.1%, where this value is used for all test cases in this paper.

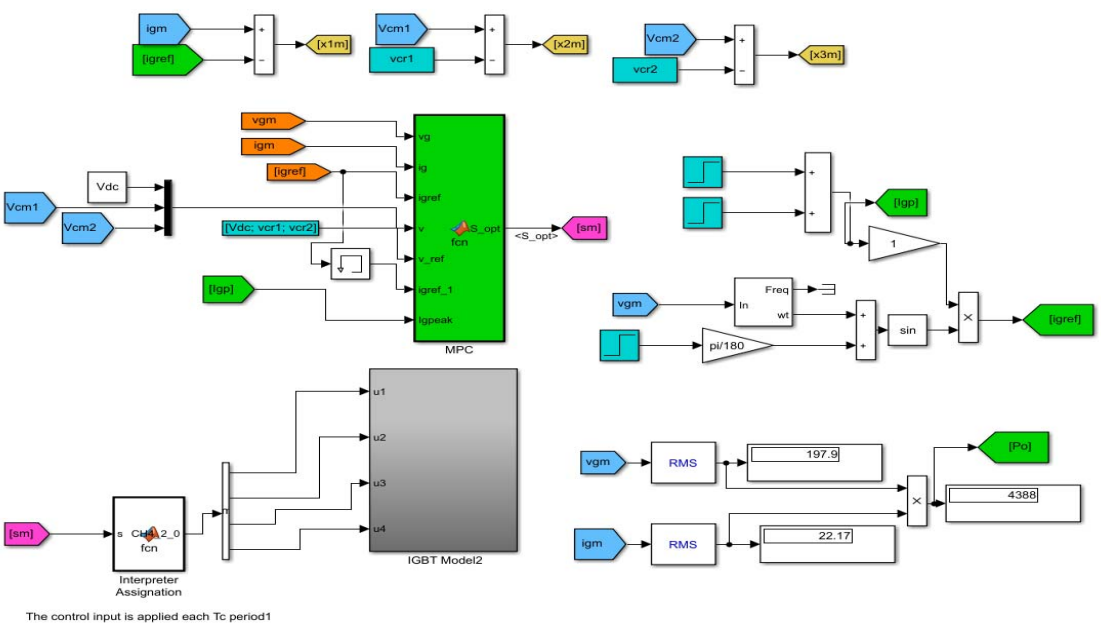

Fig.6: Complete simulation model

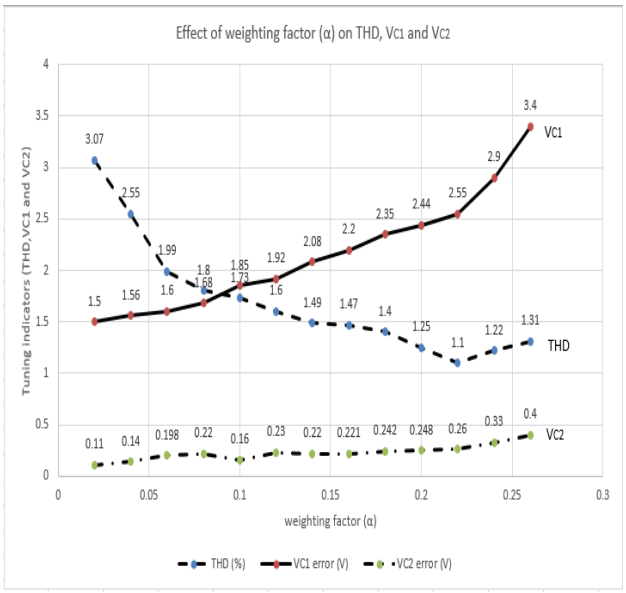

Fig.7: The effect of varying weighting factor (α) on the performance indicators

3.2 Voltage and current waveforms

To get the desired results of the proposed model, the output voltage of the inverter Vin must be greater than the grid voltage.

Fig. 8 shows the output voltage of the inverter Vin which has a peak value of 400V, while the grid voltage has a peak value of 311V. Furthermore, the 9 voltage levels are sequentially illustrated in this figure.

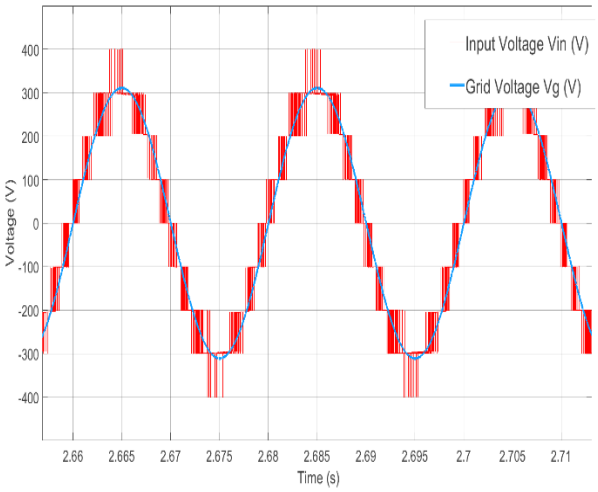

Fig.8: Voltage waveforms of the inverter and the grid

The injected current to the grid ig(t) is shown in Fig.9 with values very closed to the reference current value I_{Gref} (t). That means the THD of the current waveform is very small.

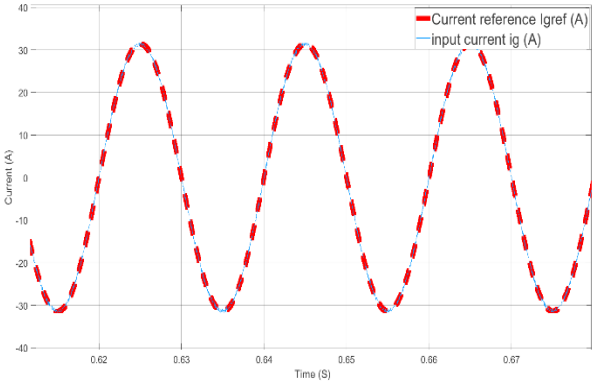

Fig.9: Injected current and reference current waveforms.

Fig. 10 illustrates the capacitors' voltages, where they are controlled as requirement around the reference values (V_{C1}= 2E = 200V and V_{C2} = E = 100V), and the steady state error of the injected current is relatively small (less than 5%) as shown on Fig.11.

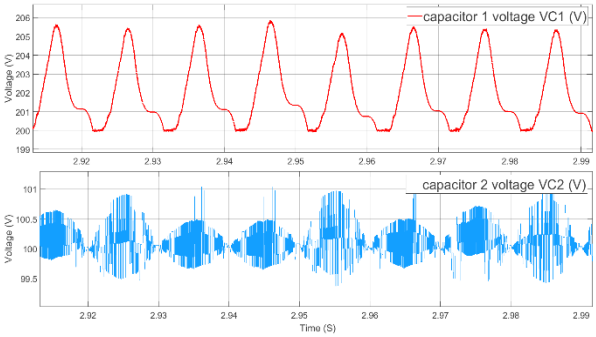

Fig.10: Capacitors' voltage waveforms

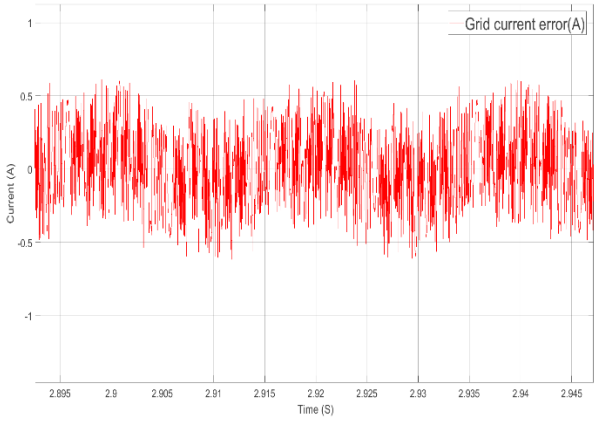

Fig.11: Injected current error.

By analyzing the output current waveform using FFT techniques, it is clear that the THD is very small (THD=1.13%) as shown on Fig.12.

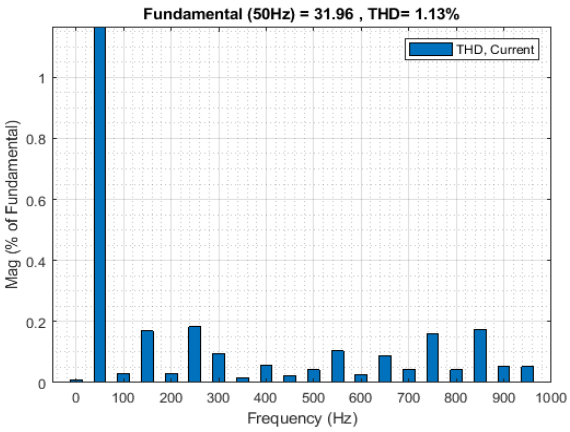

Fig.12: THD spectrum of the current,

3.3 Step change in the output power of the inverter

To study the transient operation of the inverter, a step change (at time of 0.525 S) of the injected current ig is done, where the current rises from 11.36 A to 22.72A, as shown on Fig.13, where it is clear that the response of the injected current is very fast, the capacitors' voltages error increased slightly but still relatively less than 5%, and the output power of the inverter increased from 2500 W to 5000 W within one cycle (0.02 S). While there is no change in the output voltage waveform as shown on Fig.14.

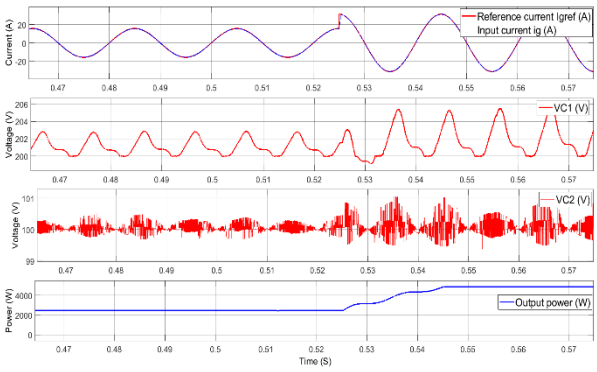

Fig.13: Injected current, V_{C1}, V_{C2}, and output power waveforms during step change in the current.

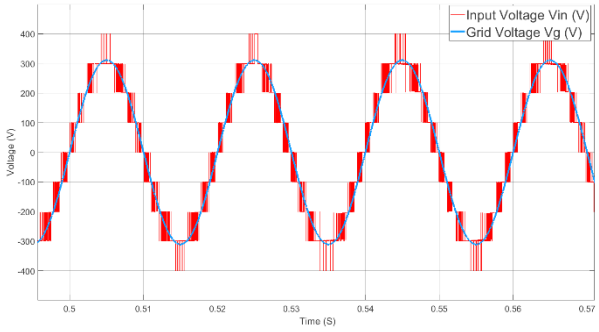

Fig.14: Voltage waveforms of inverter and grid

3.4 Robustness Analysis

In order to prove the robustness of the proposed model, the model is simulated under the effect of capacitors (C_1, C_2) and inductor filter (L_f) mismatches with grid voltage sag and swell step change. This effect is observed by changing the values of these elements from 50% to 150% of their rated values, and by changing the grid voltage from 90% to 110% of the rated value.

3.4.1 The effect of capacitors and inductor mismatches

Fig. 15 shows that if the difference in the capacitance of C_1varies between -50% and 50%, the THD is fluctuating slightly around 1.1% (but still stable) and V_{C2} remains stable around $0.3V_{RMS}$. Furthermore, there is no significant difference in the capacitance voltage ΔV_{C1} decreases from 4.9 V_{RMS} to 1.8 V_{RMS} with relatively small steady state error with values ≤ 5%.

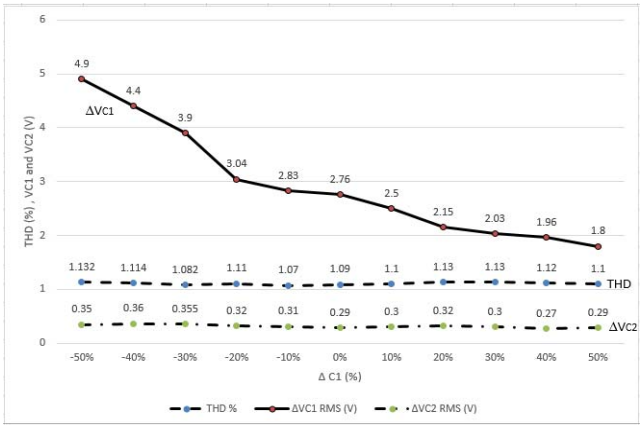

Fig.15: Effect of changing the capacitance of C_1 on the performance indicators.

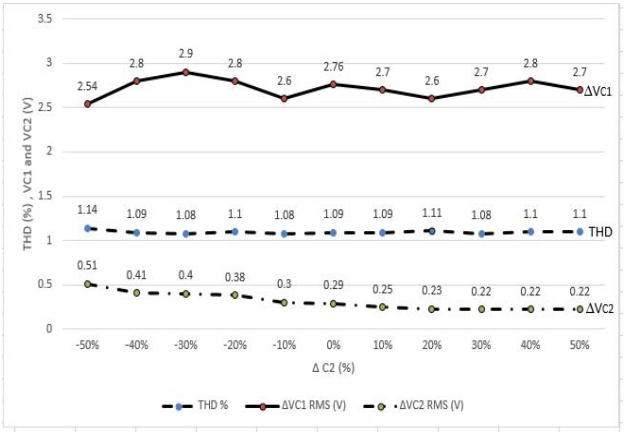

Fig.16: Effect of changing the capacitance of C_2on the performance indicators.

Fig. 16 shows that if the change of the capacitance of C_2 varies between -50% and 50%, the THD is

fluctuating slightly around 1.1% (but still stable) and ΔV_{C1} keeps stable around $2.7V_{RMS}$ with no observed difference. While ΔV_{C2} is decreasing from 0.51 V_{RMS} to 0.22 V_{RMS}, the steady state error still small with values ≤5%.

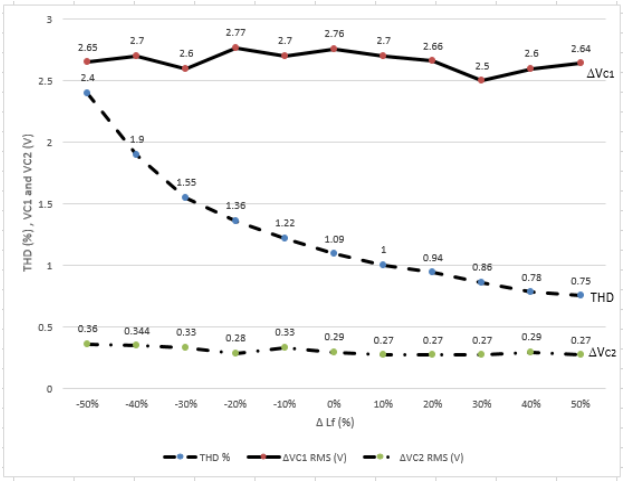

Fig.17: Effect of changing the inductance Lf on the performance indicators.

Fig. 17 illustrate the effect of changing the inductance of L_f between 50% and 150% of its rated value, where the THD decreases from 2.4% to 0.75%, ΔV_{C1} is fluctuating around $2.7V_{RMS,}$ while ΔV_{C2} to some extent keeps the same values irrespective of inductance change.

3.4.2 The effect of grid voltage sag and swell

In order to test the model robustness under grid voltage fluctuations sag and swell, a step change in the grid voltage has been applied (Vg ± 10%). An increasing of grid voltage by 10% is applied at T=0.7S and decreasing by -10% at T= 0.76S. The model stills robust, the injected current THD have no change and the capacitors' voltages are within the acceptable range.

Fig.18 shows how the input voltage changes to follow the grid voltage. Note that the model generates only seven levels at T= 0.76S due to the decreasing of grid voltage.

It's clearly shown from Fig.19 that the current injected to the grid has no change due to sag and swell of the grid voltage. The voltage error of C_1 has a slight difference but still small and within the acceptable range, while there is no observed change in the voltage error of C_2. The output power reacts heavily due to the difference of the input voltage.

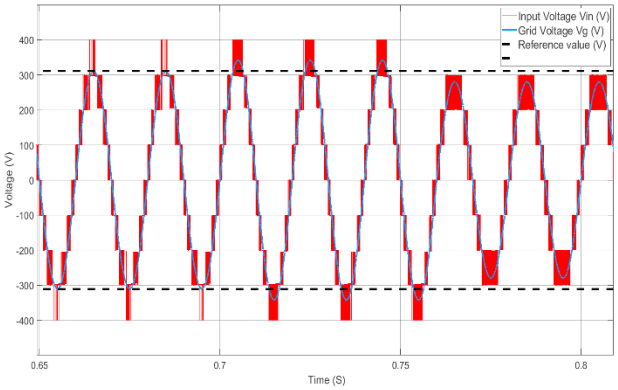

Fig.18: Voltage waveforms of inverter and grid during sag and swell voltage fluctuations.

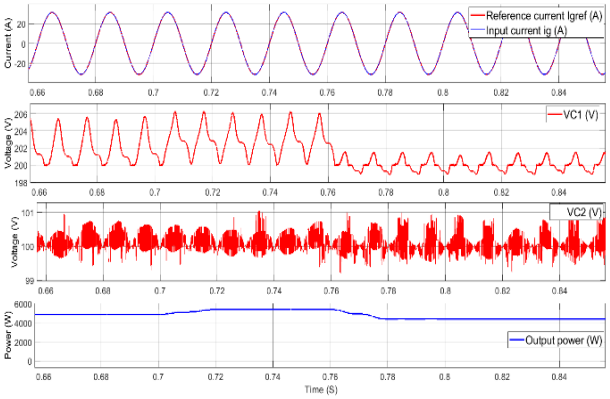

Fig.19: Injected current, V_{C1}, V_{C2}, and output power waveforms during sag and swell of grid voltage.

4 Conclusions

In this paper PUC9, multilevel inverter topology controlled by FCS-MPC technique is theoretically analyzed, mathematically modeled and simulated using MATLAB/SIMULINK software.

Simulation results show that the PUC9 can be simultaneously controlled by FCS-MPC technique. The weighting factor (α) is tuned successfully based on decreasing THD of the injected current while balancing the capacitors' voltages at their rated values.

The proposed controller behaves a stable and efficient reference current tracking and has the capability of maintaining the capacitors' voltages at their desired values during steady state and transient response.

The robustness analysis shows that the step change in the injected current, parameters' mismatching and grid voltage sag and swell does not have a significant effect on the model performances.

This study is carried out based on simulation, so this model can be experimentally implemented in order to validate the simulation results.

References:

[1] Trabelsi, M., Bayhan, S., Ghazi, K.A., Abu-Rub, H. and Ben-Brahim, L., 2016. *Finite-control-set model predictive control for grid-connected packed-U-cells multilevel inverter*. *IEEE Transactions on Industrial Electronics*, *63*(11), pp.7286-7295.

[2] Yan Zhou, Hui Li. *Analysis and Suppression of Leakage Current in Cascaded-Multilevel-Inverter-Based PV*. IEEE Transactions on industrial electronics, Vol. 29, No. 19, 2014, pp.5265-5277.

[3] Ounejjar, Y., Al-Haddad, K. and Dessaint, L.A., 2012. *A novel six-band hysteresis control for the packed U cells seven-level converter: Experimental validation*. *IEEE Transactions on Industrial Electronics*, *59*(10), pp.3808-3816.

[4] Ounejjar, Y. and Al-Haddad, K., 2010, November. *Fourteen-band hysteresis controller of the fifteen-level packed U cells converter*. In *IECON 2010-36th Annual Conference on IEEE Industrial Electronics Society* (pp. 475-480). IEEE.

[5] Sheir, A., Orabi, M., Ahmed, M.E., Iqbal, A. and Youssef, M., 2014, September. *A high efficiency single-phase multilevel packed U cell inverter for photovoltaic applications*. In *2014 IEEE 36th International Telecommunications Energy Conference (INTELEC)* (pp. 1-6). IEEE.

[6] Ounejjar, Y., Al-Haddad, K. and Gregoire, L.A., 2011. *Packed U cells multilevel converter topology: theoretical study and experimental validation*. *IEEE Transactions on Industrial Electronics*, *58*(4), pp.1294-1306.

[7] Lee, J.H., 2011. *Model predictive control: Review of the three decades of development*. International Journal of Control, Automation and Systems, 9(3), p.415.

[8] Rodriguez, J., Kazmierkowski, M.P., Espinoza, J.R., Zanchetta, P., Abu-Rub, H., Young, H.A. and Rojas, C.A., 2013. *State of the art of finite control set model predictive control in power electronics*. IEEE Transactions on Industrial Informatics, 9(2), pp.1003-1016.

[9] Guzinski, J. and Abu-Rub, H., 2013. *Speed sensorless induction motor drive with predictive current controller*. IEEE Transactions on Industrial Electronics, 60(2), pp.699-709.

[10] Rodríguez, J., Abu-Rub, H., Perez, M.A. and Kouro, S., 2014. *Application of predictive control in power electronics: An AC-DC-AC converter system.* In Advanced and Intelligent Control in Power Electronics and Drives (pp. 227-248). Springer, Cham.

[11] Trabelsi, M., Ghazi, K.A., Al-Emadi, N. and Ben-Brahim, L., 2013. *A weighted real-time predictive controller for a grid connected flying capacitors inverter.* International Journal of Electrical Power & Energy Systems, 49, pp.322-332.

[12] Rivera, M., Rodriguez, J., Espinoza, J.R. and Abu-Rub, H., 2012. *Instantaneous reactive power minimization and current control for an indirect matrix converter under a distorted ac supply*. IEEE Transactions on Industrial Informatics, 8(3), pp.482-490.

[13] Mohan, D. and Sreejith, B.K., *Performance analysis of multi level shunt active filter based on SDM*. *CiiT International Journal of Digital Signal Processing pp42-46*.

[14] Tolbert, L.M. and Peng, F.Z., 1998, February. *Multilevel converters for large electric drives*. In *APEC'98 Thirteenth Annual Applied Power Electronics Conference and Exposition*(Vol. 2, pp. 530-536). IEEE.

[15] Rodriguez, J., Lai, J.S. and Peng, F.Z., 2002. Multilevel inverters: a survey of topologies, controls, and applications. *IEEE Transactions on industrial electronics*, *49*(4), pp.724-738.

[16] Wu, B. and Narimani, M., 2017. *High-power converters and AC drives (Vol. 59*). John Wiley & Sons.

[17] Franquelo, L.G., Rodriguez, J., Leon, J.I., Kouro, S., Portillo, R. and Prats, M.A., 2008. *The age of multilevel converters*. *IEEE industrial electronics magazine*, *2*(2), pp.28-39.

[18] Kouro, S., Malinowski, M., Gopakumar, K., Pou, J., Franquelo, L.G., Wu, B., Rodriguez, J., Pérez, M.A. and Leon, J.I., 2010. *Recent advances and industrial applications of multilevel converters*. *IEEE Transactions on industrial electronics*, *57*(8), pp.2553-2580.

[19] Gupta, A.K. and Khambadkone, A.M., 2006. *A space vector PWM scheme for multilevel inverters based on two-level space vector PWM*. *IEEE Transactions on industrial electronics*, *53*(5), pp.1631-1639.

[20] Lewicki, A., Krzeminski, Z. and Abu-Rub, H., 2011. *Space-vector pulse width modulation for three-level NPC converter with the neutral point voltage control.* IEEE Transactions on Industrial Electronics, 58(11), pp.5076-5086.

[21] Cortés, P., Kazmierkowski, M.P., Kennel, R.M., Quevedo, D.E. and Rodríguez, J., 2008. *Predictive control in power electronics*

anddrives. *IEEE Transactions on industrial electronics*, *55*(12), pp.4312-4324.

[22] Kouro, S., Cortés, P., Vargas, R., Ammann, U. and Rodríguez, J., 2009. *Model predictive control—A simple and powerful method to control power* converters. *IEEE Transactions on industrial electronics*, *56*(6), pp.1826-1838.

[23] Cortés, P., Kazmierkowski, M.P., Kennel, R.M., Quevedo, D.E. and Rodríguez, J., 2008. *Predictive control in power electronics and drives*. *IEEE Transactions on industrial electronics*, *55*(12), pp.4312-4324.

[24] Rodríguez, J., Pérez, M.A., Young, H. and Abu-Rub, H., 2014. *Model predictive speed control of electrical machines*. Power Electronics for Renewable Energy Systems, Transportation and Industrial Applications,

[25]Trabelsi, M., Ghazi, K.A., Al-Emadi, N. and Ben-Brahim, L., 2012, October. *An original controller design for a grid connected PV system.* In IECON 2012-38th Annual Conference on IEEE Industrial Electronics Society (pp. 924-929). IEEE.

[26] Marcelo A. Pérez, Patricio Cortés, and José Rodríguez, *Predictive Control Algorithm Technique for Multilevel Asymmetric Cascaded H-Bridge Inverters*, IEEE Transactions on Industrial Electronics, Vo.55, No.12, 2008, pp.4354-4361.

[27] https://www.mathworks.com, matlabcentral, 354951-matlab-r2016b .